nature climate change

LETTERS

PUBLISHED ONLINE: 31 AUGUST 2015 | DOI: 10.1038/NCLIMATE2769

Climate velocity and the future global redistribution of marine biodiversity

Jorge García Molinos[1,2*], Benjamin S. Halpern[3,4,5], David S. Schoeman[6], Christopher J. Brown[7], Wolfgang Kiessling[8,9], Pippa J. Moore[10,11], John M. Pandolfi[12], Elvira S. Poloczanska[7,13], Anthony J. Richardson[13,14] and Michael T. Burrows[1]

Anticipating the effect of climate change on biodiversity, in particular on changes in community composition, is crucial for adaptive ecosystem management[1] but remains a critical knowledge gap[2]. Here, we use climate velocity trajectories[3], together with information on thermal tolerances and habitat preferences, to project changes in global patterns of marine species richness and community composition under IPCC Representative Concentration Pathways[4] (RCPs) 4.5 and 8.5. Our simple, intuitive approach emphasizes climate connectivity, and enables us to model over 12 times as many species as previous studies[5,6]. We find that range expansions prevail over contractions for both RCPs up to 2100, producing a net local increase in richness globally, and temporal changes in composition, driven by the redistribution rather than the loss of diversity. Conversely, widespread invasions homogenize present-day communities across multiple regions. High extirpation rates are expected regionally (for example, Indo-Pacific), particularly under RCP8.5, leading to strong decreases in richness and the anticipated formation of no-analogue communities where invasions are common. The spatial congruence of these patterns with contemporary human impacts[7,8] highlights potential areas of future conservation concern. These results strongly suggest that the millennial stability of current global marine diversity patterns, against which conservation plans are assessed, will change rapidly over the course of the century in response to ocean warming.

Climate change is expected to become the greatest driver of change in global biodiversity in the coming decades[9]. To avoid extinction, organisms exposed to a changing climate can respond by adapting to the new conditions within their current range or by dynamically tracking their climatic niches in space (distribution shifts) or time (phenological shifts). Although the evolutionary potential for marine organisms to cope with climate change remains uncertain[10], distribution shifts are already widely observed[11–13] and are likely to become increasingly important, given the expected intensification of current rates of climate change[14].

Forecasting climate-driven distribution shifts is challenging because they frequently depart from expected patterns of simple poleward movement[13]. However, recent evidence suggests that local climate velocity[15], a measure of the speed and direction of migrating isotherms, is a useful and simple predictor of the rate and direction of shift across a wide variety of marine taxa[11,12,16]. Here we use trajectories of climate velocity[3] to predict global marine biodiversity patterns at 1° resolution under future anthropogenic climate change. Previous attempts to globally project biogeographical shifts of marine species in response to climate change[5,6,17] have all been based on the bioclimatic-niche and population-dynamics model developed by Cheung and colleagues[5]. These are limited to sufficiently well-studied, commercially exploited species, and focus on changes in species richness. Our simple, intuitive model allows us instead to model an order of magnitude more species, spanning a wide range of taxonomic groups (12,796 marine species from 23 phyla; Supplementary Table 1). Importantly, our analysis is not limited to changes in species richness but, for the first time, looks into the effect of climate change on spatio-temporal patterns in community composition at a global scale (see Methods). Finally, to contextualize our projections to current human pressures on biodiversity, we explore the spatial congruence between future anthropogenic climate change impacts, as suggested by our projections, and the degree of contemporary human impacts on the ocean[8].

On the basis of modelled species distribution data[18], we projected shifts in current thermal niche space for each species by calculating the trajectory that isotherms will follow up to 2100 based on RCPs 4.5 and 8.5 (Supplementary Table 2 and Supplementary Fig. 1), integrating through time the spatial variation in the magnitude and direction of local climate velocities (see Methods and Supplementary Fig. 2). Occupancy within the new domain was determined thereafter as a function of thermal and habitat suitability, in terms of depth and coastal affinity, for each species (Supplementary Figs 3–5). Our projections of range shifts refer exclusively to those expected in response to changes in

[1]Scottish Association for Marine Science, Oban, Argyll PA37 1QA, UK. [2]Center for Environmental Biology and Ecosystem Studies, National Institute for Environmental Studies, 16-2 Onogawa, Tsukuba, Ibaraki 305-8506, Japan. [3]Bren School of Environmental Science and Management, University of California, Santa Barbara, California 93106, USA. [4]Imperial College London, Silwood Park Campus, Buckhurst Road, Ascot SL5 7PY, UK. [5]NCEAS, 735 State St., Santa Barbara, California 93101, USA. [6]School of Science and Engineering, University of the Sunshine Coast, Maroochydore, Queensland 4558, Australia. [7]The Global Change Institute, The University of Queensland, Brisbane, Queensland 4072, Australia. [8]GeoZentrum Nordbayern, Paläoumwelt, Universität Erlangen-Nürnberg, Loewenichstrasse 28, 91054 Erlangen, Germany. [9]Museum für Naturkunde, Invalidenstrasse 43, 10115 Berlin, Germany. [10]Institute of Biological, Environmental and Rural Sciences, Aberystwyth University, Aberystwyth SY23 3DA, UK. [11]Centre for Marine Ecosystems Research, Edith Cowan University, Perth 6027, Australia. [12]School of Biological Sciences, Australian Research Council Centre of Excellence for Coral Reef Studies, The University of Queensland, Brisbane, Queensland 4072, Australia. [13]CSIRO Oceans and Atmosphere Flagship, Ecosciences Precinct, Boggo Road, Brisbane, Queensland 4001, Australia. [14]Centre for Applications in Natural Resource Mathematics (CARM), School of Mathematics and Physics, The University of Queensland, St Lucia, Queensland 4072, Australia. *e-mail: jorge.garcia@nies.go.jp

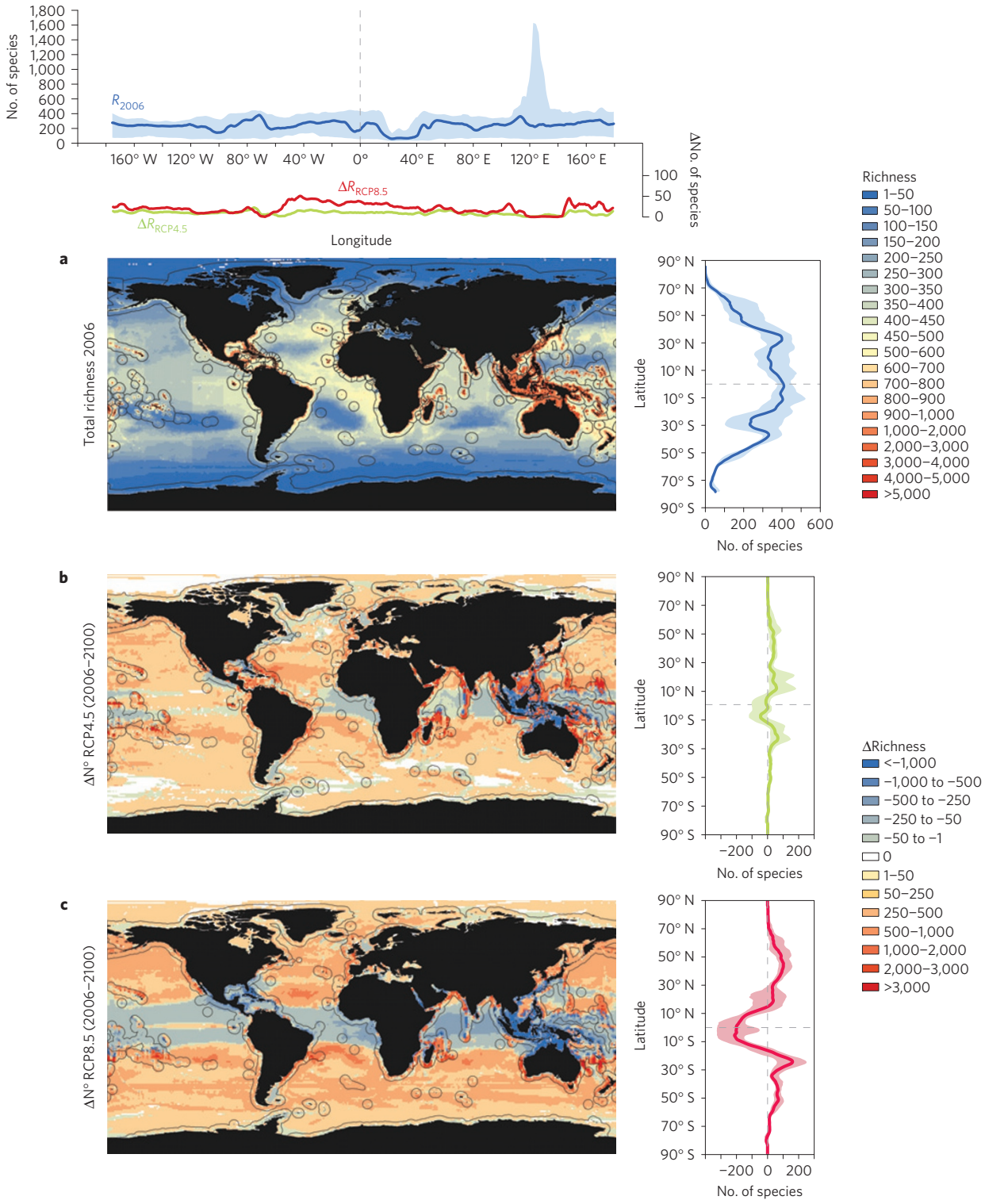

Figure 1 | Redistribution of global biodiversity patterns under future climate change. a, Total current species richness ($n = 12{,}796$). **b**,**c**, Differences between current (year 2006) and projected (year 2100) cell species richness for Representative Concentration Pathways (RCPs) RCP4.5 (**b**) and RCP8.5 (**c**). Black contour lines correspond to limits of exclusive economic zones (EEZ). Latitudinal and longitudinal global medians (solid line) with their 25 and 75% quartiles (shaded area) (5° moving average) are given in the marginal panels to the right and above, respectively.

mean sea surface temperature (SST). Whereas other temperature parameters might be better predictors for species living far from the sea surface, SST has been shown to be a consistent significant predictor of marine species richness across taxonomic groups[19] frequently linked to observed distribution shifts[11], including those for benthic species[16]. Our model also relies on rough estimates of thermal breadths, based on absolute temperature extremes within a species range, which are likely to yield conservative projections, in particular for cosmopolitan species with wide distributions (for example, compare panels c and d in Supplementary Fig. 5). Therefore, results should be interpreted with all these caveats in mind (see Supplementary Methods and Supplementary Discussion for a

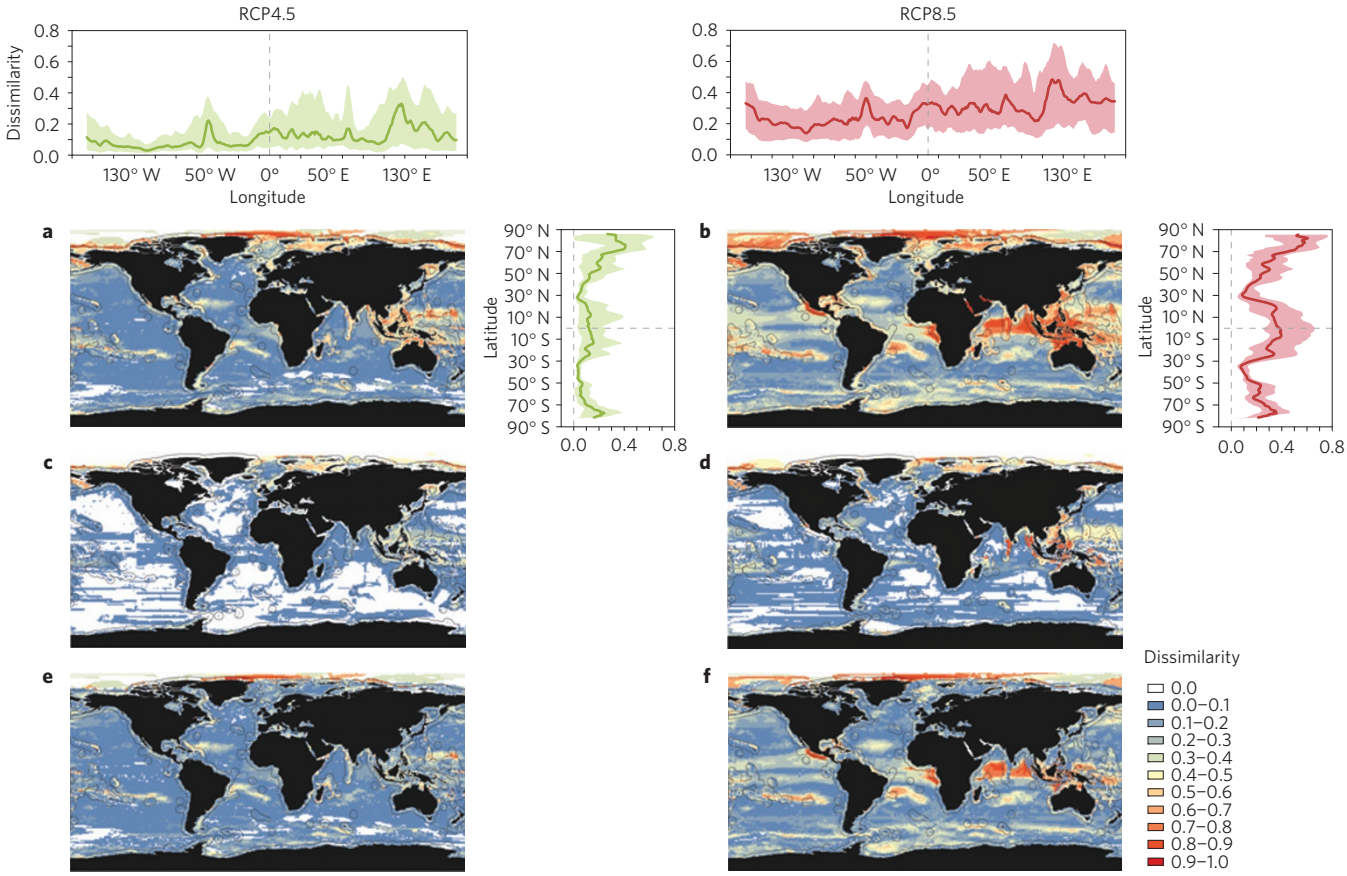

Figure 2 | Partitioning of cell-based temporal β-diversity under future climate change. a,**b**, Patterns in total β-diversity expressed as cell-based Sørensen dissimilarities (0 = no dissimilarity) between present-day (2006) communities and those projected for 2100. **c**–**f**, Corresponding additive decomposition of **a**,**b** into true temporal turnover (that is, species replacement) (**c**,**d**) and nestedness (that is, either extirpations or invasions, not both) (**e**,**f**). **a**,**c**,**e** are for RCP4.5 and **b**,**d**,**f** are for RCP8.5. Black contour lines correspond to exclusive economic zones (EEZ) limits.

detailed account on the assumptions and uncertainties associated with our model). The outcome of climate change on biodiversity clearly depends on additional abiotic and biotic factors, including human impacts. Global warming nevertheless imparts a distinctive fingerprint of climate change on our oceans, unequivocally linked to species distribution shifts[11,12]. Our analysis thus provides the simplest expectation for the future redistribution of biodiversity.

Our model predicts strong changes in global patterns of species richness (Fig. 1a), robust to underlying variability in projected SST (Supplementary Fig. 6), with contrasting outcomes between climate-change scenarios and considerable regional variability (Fig. 1b,c and Supplementary Fig. 7). These results are in general agreement with previously predicted patterns[5,6], highlighting the pivotal role of temperature on species distribution shifts and supporting the adequacy of our model. Although similar in the short-term (Supplementary Fig. 7), patterns of invasion and extirpation under both RCPs diverge in mid-century (2040–2065), which under RCP8.5 is a period of transition from a prevailing net gain to a net loss of biodiversity. Overall, projections from RCP8.5 (2006–2100) show a latitudinal peak in net richness gain at ~40/30° N/S, and widespread areas of richness loss near the equator, concentrated in the Central Indo-Pacific (Fig. 1c). This pattern is consistent with that inferred from palaeontological records during past episodes of rapid climate warming[20]. High rates of extirpation are expected for equatorial species under moderate warming (2–3 °C; ref. 21) given their narrow thermal tolerance ranges and comparatively low capacity for acclimatization[22]. Projected extirpations, but not invasions, were sensitive to the criteria used to estimate the upper thermal tolerances of species (see also Supplementary Fig. 5), although general spatial patterns remained unaltered (see Supplementary Methods and Supplementary Fig. 8). In contrast to those under RCP8.5, net losses under RCP4.5 are projected to be low by 2100 (Fig. 1b), with the latitudinal peak in richness located at lower latitudes (~20° N–S; Fig. 1b); a pattern resulting from the net overriding effect of species invasions relative to local extinctions, except in the tropics (Supplementary Fig. 7).

Changes in composition of present communities are projected to be large by 2100 across the Arctic, the tropics, particularly the Indo-Pacific, and some temperate (for example, North Sea) and Southern Ocean regions (Fig. 2a,b). These changes are much more intense and widespread under RCP8.5 (Fig. 2b) than RCP4.5 (Fig. 2a), mainly driven by the invasion of species into local communities without loss (except in the tropics) of resident species (that is, nestedness; Fig. 2e,f), and by temporal turnover in the Central Indo-Pacific and the Arctic (that is, species replacement; Fig. 2c,d). Recent evidence suggests that the systematic loss of species is not a global driver of the temporal change in composition of present-day communities[2]; we predict this will hold into the future. Although extinctions are projected to be regionally important (Supplementary Fig. 7), it is their combination with the invasion of species that ultimately drives the turnover of communities (Fig. 2c,d). The intense replacement of species, mainly within the Central Indo-Pacific, may lead to the formation of no-analogue assemblages, resulting in novel species associations and interactions[23]. Extensive areas experiencing little or no change in community composition by 2100 also occur (19% and 54% of marine cells with total dissimilarity < 0.1 for RCP8.5 and RCP4.5, respectively; Fig. 2a,b). These are areas of low climate change velocity (Supplementary Fig. 2), with strong

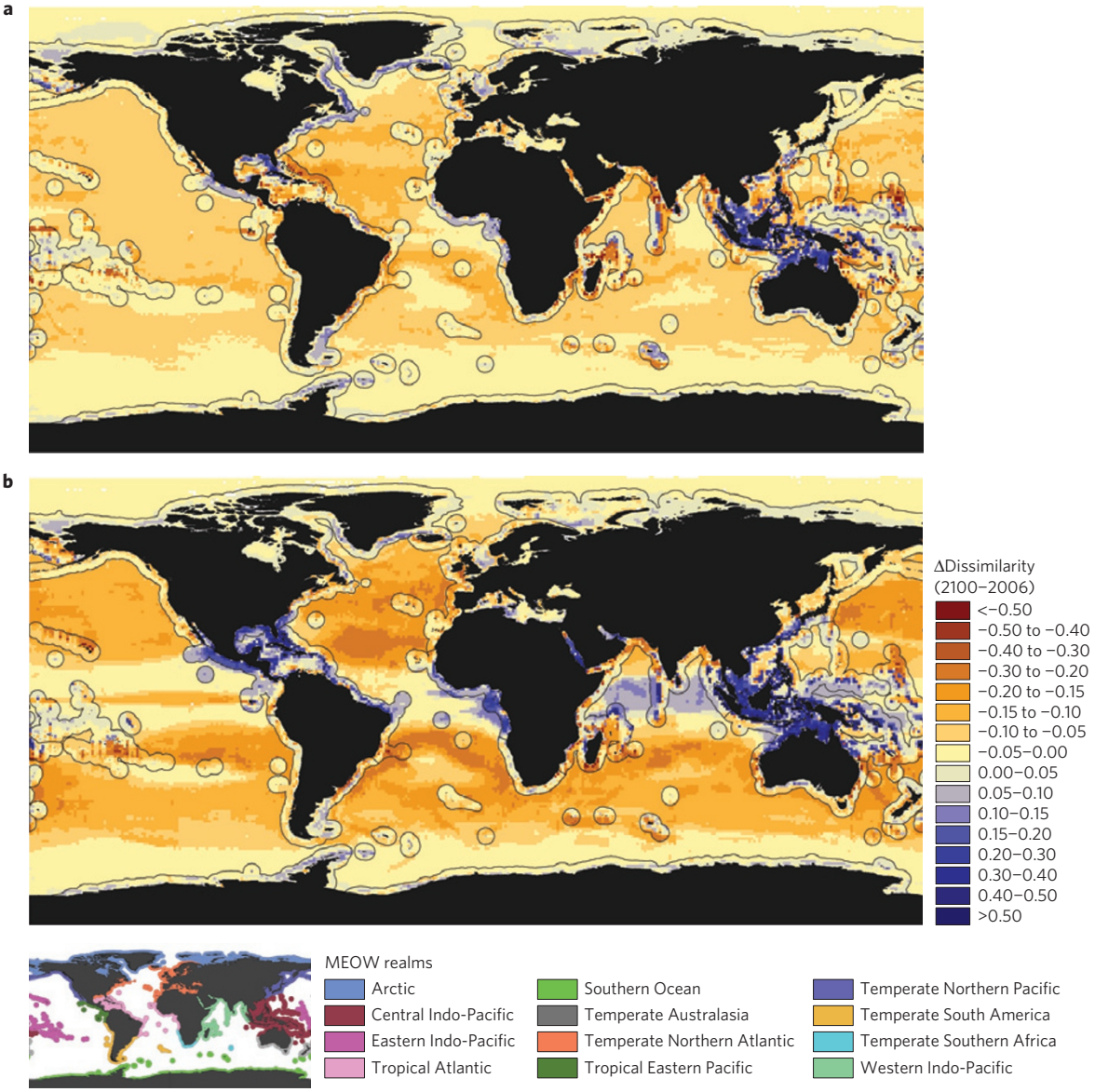

Figure 3 | Spatial homogenization of present-day communities under future climate change. a,**b**, Projected 2006–2100 spatial variation in Sørensen dissimilarities between cell-based communities and the regional species pool, comprising all species present within the corresponding Marine Ecoregions of the World (MEOW) realm and the High Seas, between 2006 and 2100 for RCP4.5 (**a**) and RCP8.5 (**b**). Negative values denote a decrease in dissimilarity (that is, increased spatial homogenization). Black lines represent MEOW realm limits as identified in the lower panel (the white area corresponding to the High Seas region).

temperature gradients or with stable future climatic conditions, which make them potential sites for protecting stable communities[3]. In the absence of extirpations, widespread invasions will cause a strong spatial biotic homogenization of present-day communities (Fig. 3), where locations within regions will share an increased number of species. This homogenization effect contrasts with both the projected increase in alpha diversity (Fig. 1) and temporal changes in beta diversity (Fig. 2) on local communities. However, regional beta diversity will increase for those areas where large numbers of species are extirpated (for example, the tropics). Although the outcome of invasions on biodiversity will depend on the nature of the interaction between invasive and resident species[24], our results highlight regions where such interactions are likely to be stronger under future climate change and could be considered for inclusion in adaptive management programmes.

Comparison of projected (2006–2100) changes in species richness and community composition with contemporary (1985–2005) cumulative human impact[7,8] averaged across individual exclusive economic zones (EEZs) and sovereign regions highlights potential areas of conservation relevance for marine governance (Fig. 4 and Supplementary Fig. 9 and Supplementary Table 3). Overlap between high current human impact and large future changes in biodiversity occurs under both RCPs within EEZs of the eastern Mediterranean (Cyprus, Greece, Malta), northwestern Atlantic (Iceland, Faeroe Islands, UK), and multiple tropical and subtropical regions, such as the Caribbean (Antigua and Barbuda, Anguilla), Madagascar, and northwestern areas of Africa (Morocco, Mauritania) and the Central Indo-Pacific (Northern Mariana, Philippines, Taiwan, China). These areas should be considered for mitigation and restoration actions directed at reducing existing levels of other human impacts, building resilience to the effects of climate change. Among these regions, the Coral Triangle and neighbouring EEZs emerge as unique in that the largest biodiversity losses and changes in composition associated with both RCPs can

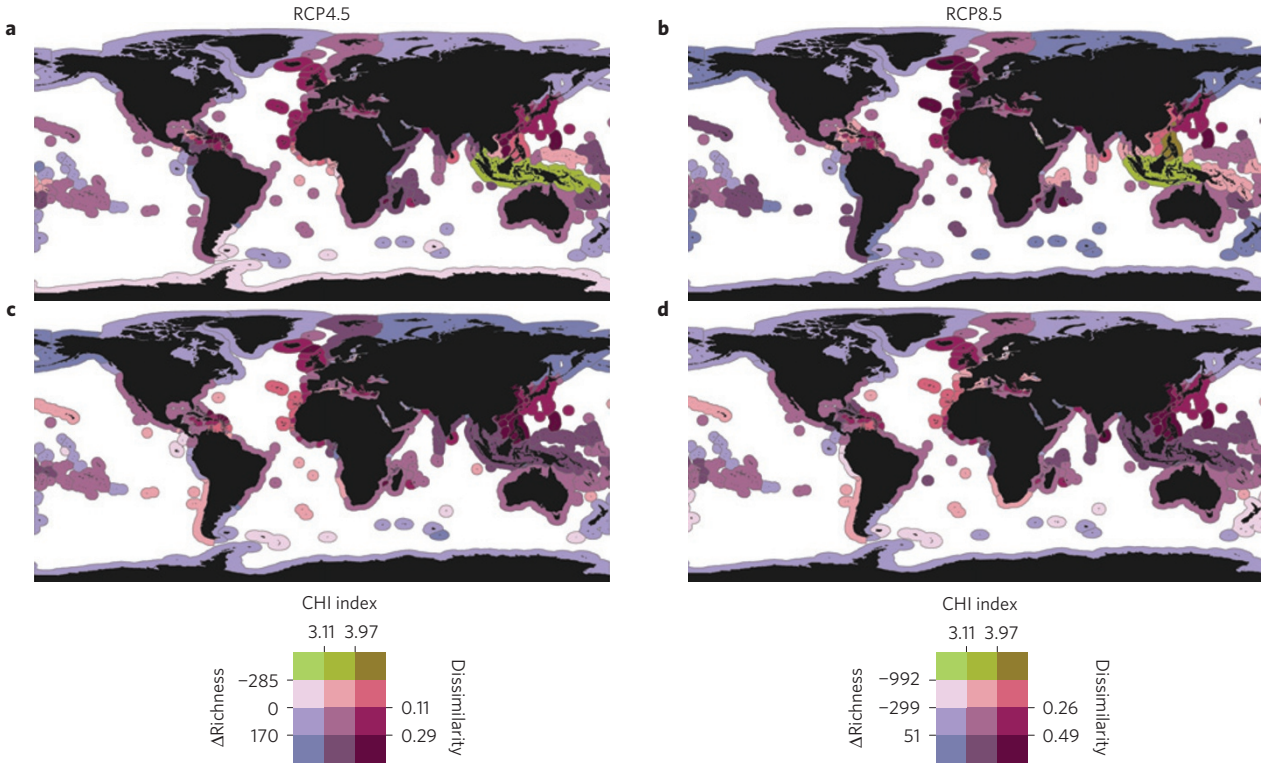

Figure 4 | Projected changes in species richness and community composition in relation to contemporary human impacts. a–d, Choropleth maps showing relationships between contemporary mean cumulative human impact index (CHI)[7,8] and projected (2006–2100) mean differences in total richness (**a**,**b**) and mean composition dissimilarities (total temporal β-diversity) (**c**,**d**) within EEZ regions for RCP4.5 (**a**,**c**) and RCP8.5 (**b**,**d**). Colour category breaks correspond to the 25th and 75th percentiles for each variable, with the exception of total richness for the RCP8.5, which also includes the 5th percentile to highlight EEZs (primarily in the Coral Triangle) with a high net decrease in richness. Refer to Supplementary Table 3 for a detailed account by EEZ.

be expected. The fact that several of these EEZ 'hotspots' include some of the world's most vexing maritime territorial disputes (for example, Senkaku, Paracel and Spratly islands, located in the East and South China seas) highlights the complex role that climate change might have for international ocean governance. The likely arrival of large numbers of climate migrants, and resulting compositional changes in present-day biotic communities, could exacerbate tensions and strain negotiations over sovereignty, with uncertain global repercussions[25]. At the other extreme, several EEZs at present experiencing low anthropogenic impact, including high-latitude EEZs (Russia, Alaska, Canada, Antarctica), are projected to experience relatively large changes in community composition (Fig. 4). These are areas where proactive conservation efforts directed towards preserving and protecting the integrity and functioning of current ecosystems might be considered more appropriate than maintenance of individual species.

With current emissions tracking slightly above RCP8.5, preventing an increase in global temperature over 2 °C seems increasingly unlikely[14]. Both empirical[21] and modelled[5] evidence suggests that impacts of global warming on marine biodiversity are likely to be markedly different within a very narrow margin of temperature increase. Although our results support this hypothesis, they also suggest a widespread redistribution of current biodiversity regardless of the scenario followed. In the past, centres of global marine biodiversity have shifted in location over geologic timescales, mainly driven by major tectonic events[26], with current biodiversity patterns being established well before the Pleistocene over 2.5 million years ago. Our projections, however, suggest strongly that anthropogenic climate change will drive generalized changes in the global distribution of marine species over the course of a century.

Although the ability of marine ectotherms to track their shifting thermal niches by expanding their ranges will depend on a number of factors[27], including finding suitable colonization conditions[28], our results de-emphasize global biodiversity loss attributed directly to anthropogenic ocean warming, but highlight the likely future biotic homogenization of marine communities, with resultant novel biotic interactions. Changing species interactions rather than warming per se are an important cause of documented population declines and extinctions related to climate change[29]. Current conservation plans will therefore need to anticipate and accommodate such changes, unprecedented in human history. Our results also reinforce current concerns over global warming and ocean governance[30], and their potential effects on the spatial mismatch between scales of governance and ecosystem conservation. Because effects of climate change will transcend jurisdictional borders, proactive conservation efforts should be made at adequate scales of governance through effective marine spatial planning, including, for example, promoting regional conservation frameworks for cross-country cooperation.

Note added in proof: As this manuscript was being prepared for publication, a related theoretical study[31] appeared that projects changes in the distributions of 'pseudo-species' in response to warmer oceans, and reaches some conclusions similar to our own.

Methods

Methods and any associated references are available in the online version of the paper.

Received 29 July 2014; accepted 25 July 2015;
published online 31 August 2015

References

1. Hannah, L. *et al.* Global climate change adaptation priorities for biodiversity and food security. *PLoS ONE* **8,** e72590 (2013).

2. Dornelas, M. *et al.* Assemblage time series reveal biodiversity change but not systematic loss. *Science* **344,** 296–299 (2014).
3. Burrows, M. T. *et al.* Geographical limits to species-range shifts are suggested by climate velocity. *Nature* **507,** 492–495 (2014).
4. Moss, R. H. *et al.* The next generation of scenarios for climate change research and assessment. *Nature* **463,** 747–756 (2010).
5. Cheung, W. W. L. *et al.* Projecting global marine biodiversity impacts under climate change scenarios. *Fish Fish.* **10,** 235–251 (2009).
6. Jones, M. C. & Cheung, W. W. L. Multi-model ensemble projections of climate change effects on global marine biodiversity. *ICES J. Mar. Sci.* **72,** 741–752 (2014).
7. Halpern, B. S. *et al.* Spatial and temporal changes in cumulative human impacts on the world's ocean. *Nature Commun.* **6,** 7615 (2015).
8. Halpern, B. S. *et al.* A global map of human impact on marine ecosystems. *Science* **319,** 948–952 (2008).
9. Leadley, P. *et al. Biodiversity Scenarios: Projections of 21st Century Change in Biodiversity and Associated Ecosystem Services* Report No. 92-9225-219-4 (Montreal, Canada: Secretariat of the Convention on Biological Diversity, 2010).
10. Munday, P. L., Warner, R. R., Monro, K., Pandolfi, J. M. & Marshall, D. J. Predicting evolutionary responses to climate change in the sea. *Ecol. Lett.* **16,** 1488–1500 (2013).
11. Poloczanska, E. S. *et al.* Global imprint of climate change on marine life. *Nature Clim. Change* **3,** 919–925 (2013).
12. Pinsky, M. L., Worm, B., Fogarty, M. J., Sarmiento, J. L. & Levin, S. A. Marine taxa track local climate velocities. *Science* **341,** 1239–1242 (2013).
13. Chen, I.-C., Hill, J. K., Ohlemüller, R., Roy, D. B. & Thomas, C. D. Rapid range shifts of species associated with high levels of climate warming. *Science* **333,** 1024–1026 (2011).
14. Peters, G. P. *et al.* The challenge to keep global warming below 2 °C. *Nature Clim. Change* **3,** 4–6 (2013).
15. Burrows, M. T. *et al.* The pace of shifting climate in marine and terrestrial ecosystems. *Science* **334,** 652–655 (2011).
16. Hiddink, J. G., Burrows, M. T. & García Molinos, J. Temperature tracking by North Sea benthic invertebrates in response to climate change. *Glob. Change Biol.* **21,** 117–129 (2014).
17. Pereira, H. M. *et al.* Scenarios for global biodiversity in the 21st century. *Science* **330,** 1496–1501 (2010).
18. Kaschner, K. *et al. AquaMaps: Predicted Range Maps for Aquatic Species* Version 08/2013 (2013); http://www.aquamaps.org
19. Tittensor, D. P. *et al.* Global patterns and predictors of marine biodiversity across taxa. *Nature* **466,** 1098–1101 (2010).
20. Kiessling, W., Simpson, C., Beck, B., Mewis, H. & Pandolfi, J. M. Equatorial decline of reef corals during the last Pleistocene interglacial. *Proc. Natl Acad. Sci. USA* **109,** 21378–21383 (2012).
21. Nguyen, K. D. T. *et al.* Upper temperature limits of tropical marine ectotherms: Global warming implications. *PLoS ONE* **6,** e29340 (2011).
22. Somero, G. N. The physiology of climate change: How potentials for acclimatization and genetic adaptation will determine 'winners' and 'losers'. *J. Exp. Biol.* **213,** 912–920 (2010).
23. Blois, J. L., Zarnetske, P. L., Fitzpatrick, M. C. & Finnegan, S. Climate change and the past, present, and future of biotic interactions. *Science* **341,** 499–504 (2013).
24. Araújo, M. B. & Luoto, M. The importance of biotic interactions for modelling species distributions under climate change. *Glob. Ecol. Biogeogr.* **16,** 743–753 (2007).
25. Koo, M. G. *Island Disputes and Maritime Regime Building in East Asia* (Springer, 2009).
26. Renema, W. *et al.* Hopping hotspots: Global shifts in marine biodiversity. *Science* **321,** 654–657 (2008).
27. Keith, S. A., Baird, A. H., Hughes, T. P., Madin, J. S. & Connolly, S. R. Faunal breaks and species composition of Indo-Pacific corals: The role of plate tectonics, environment and habitat distribution. *Proc. R. Soc. B* **280,** 20130818 (2013).
28. Deutsch, C., Ferrel, A., Seibel, B., Pörtner, H.-O. & Huey, R. B. Climate change tightens a metabolic constraint on marine habitats. *Science* **348,** 1132–1135 (2015).
29. Cahill, A. E. *et al.* How does climate change cause extinction? *Proc. R. Soc. B* **280,** 20121890 (2013).
30. Craig, R. K. Ocean governance for the 21st century: Making marine zoning climate change adaptable. *Harv. Environ. Law Rev.* **36,** 305–350 (2012).
31. Beaugrand, G., Edwards, M., Raybaud, V., Goberville, E. & Kirby, R. R. Future vulnerability of marine biodiversity compared with contemporary and past changes. *Nature Clim. Change* **5,** 695–701 (2015).

Acknowledgements

J.G.M., M.T.B., and P.J.M. were supported by the UK National Environmental Research Council grant NE/J024082/1. J.G.M. thanks the additional support received from the International Research Fellow Programme of the Japan Society for the Promotion of Science (JSPS/FF1/434). D.S.S. and J.M.P. were respectively supported by the Australian Commonwealth's Collaborative Research Network and the Australian Research Council's Centre of Excellence for Coral Reef Studies. We acknowledge the World Climate Research Programme's Working Group on Coupled Modelling, responsible for CMIP, and thank the groups (Supplementary Table 1) for producing and making available their model output.

Author contributions

J.G.M. and M.T.B. conceived the research and developed the model. B.S.H. provided species distribution and cumulative human impact data. J.G.M. conducted the analysis. All authors contributed to discussion of ideas and J.G.M. drafted the paper with substantial input from all authors.

Additional information

Supplementary information is available in the online version of the paper. Reprints and permissions information is available online at www.nature.com/reprints. Correspondence and requests for materials should be addressed to J.G.M.

Competing financial interests

The authors declare no competing financial interests.

Methods

Climate data and velocity of climate change. We used projected (2006–2100) mean annual sea surface temperature (SST) data from multi-model ensemble means (Supplementary Table 2) for two IPCC Representative Concentration Pathways[4] (RCPs): RCP4.5 and RCP8.5. RCP8.5 represents a rising pathway scenario characterized by an increasing greenhouse gas emission trajectory over time (Supplementary Fig. 1), working on the assumption of a $>8.5\,W\,m^2$ radiative forcing by 2100 relative to pre-industrial values. RCP4.5 represents an 'emissions stabilization' scenario where total radiative forcing is stabilized at $\sim 4.5\,W\,m^2$ shortly after 2100 and in which temperatures rise at a rate comparable to that of the RCP8.5 during the first decades of the century, but slow progressively thereafter (Supplementary Fig. 1). RCP8.5 yields the highest rates of warming, with global mean sea surface temperature in 2100 increasing by 2.4 °C relative to 2006 levels (corresponding ocean warming of 1 °C is expected for RCP4.5). Ensemble means were extracted from the Royal Netherlands Meteorological Institute Climate Explorer portal (http://climexp.knmi.nl) based on individual model outputs sourced from the Coupled Model Intercomparison Project phase 5 (CMIP5).

To account for the differences in the rate of change in temperature, and hence climate velocity, over time we distinguished three climate change projection periods within each climate change scenario: early (2006–2040), mid (2041–2065) and late (2066–2100) twenty-first century. Thresholds between periods were set to accommodate detected statistically significant ($\alpha = 0.05$) changes in SST linear trend in both climate scenarios using the generic change-detection algorithm for time series BFAST (Breaks For Additive Seasonal and Trend; ref. 32; Supplementary Fig. 1). Global 1°-resolution climate velocity ($°C\,km^{-1}$) maps (Supplementary Fig. 2) were produced for each combination of climate change period and climate scenario by dividing the corresponding SST linear trend ($°C\,yr^{-1}$) by the spatial gradient ($°C\,km^{-1}$) using the associated spatial angles as an estimate of direction[15].

Species distribution maps. Modelled species distribution data (Supplementary Table 1) were extracted from AquaMaps[18]. AquaMaps maps predict relative probabilities of species occurrence (0–1 range) derived from an environmental niche envelope model supplemented with species-specific information from occurrence records and, where available, expert knowledge (6.6% of the maps available as for 8 December 2014). Transfer of these probabilities into presence/absence range maps implicitly ignores niche suitability information, which can overestimate the range of cosmopolitan species in marginally suitable areas (for example, truly oceanic species on shelf areas). This effect is customarily controlled by imposing a probability threshold on species presence, restricting their resulting range to those regions of high environmental suitability (that is, the core range). Important to the type of analysis conducted here, previous studies using data sets sourced from AquaMaps have demonstrated that resulting global biodiversity patterns are largely insensitive to this parameter for moderate thresholds (<0.5; refs 6,33). In general, ranges of widespread generalists, associated with multiple environments with different probability of occurrence, are the most affected, whereas endemic or habitat specialists are relatively insensitive because they have a high probability of occurrence across their entire range. Here we used an arbitrary minimum threshold of 0.4, resulting in an overall range reduction of $-24 \pm 14\%$ (mean $\pm$ 1 s.d.) from that generated by using a non-exclusive approach (species presence defined by probability of occurrence > 0), with considerable among-phyla variation (Supplementary Table 1).

Resulting distribution maps (0.5°-resolution) were subsequently up-scaled to match the 1°-resolution of the climate data by applying a $\geq$50% cell occupancy criterion (that is, two or more of the four 0.5° cells occupied). This is a subjective, although pragmatic, choice that exclusively affects cells at the range edges and depends on the actual shape of the distribution range (for example, range variation higher for convoluted than regular shapes). Relative to ranges defined by the adopted 0.5 threshold, the use of a more conservative (four cells out of four) or inclusive (one cell out of four) criterion resulted in mean range variations across all taxa of $-61 \pm 20\%$ and $24 \pm 9\%$, respectively.

Environmental temperature extremes and taxon thermal tolerance limits. Environmental temperature extremes for each projected period were defined from the multi-model ensemble mean SST data as the maximum and minimum mean monthly SST within that period for each climate scenario. Species' thermal tolerance limits were estimated from the 1°-resolution HadISST 1.1 global SST baseline (1979–2009) climatology as one standard deviation above/below the inter-annual mean of the absolute annual maximum/minimum mean monthly SST within the species' current range (Supplementary Fig. 3). Given the lack of experimental data for most of the species, our definition of the thermal tolerance limits is subjective but pragmatic. Specifically, it intends to incorporate the potential effect of historical variability in mean SST: the greater the magnitude of temperature variation within a species' range, the wider physiological windows are expected to be in ectothermic animals (that is, the climate variability hypothesis)[34]. Sensitivity analysis to examine how the selection of more (that is, $\pm$2 s.d.) or less (that is, using only the mean) conservative thermal limits would influence model outputs (Supplementary Fig. 8) showed that, whereas patterns of leading-edge expansions (that is, invasions) remained unaltered irrespective of the minimum thermal limit chosen (results not shown), selection of the maximum thermal limit strongly influenced the number of trailing-edge contractions (that is, extirpations), particularly under RCP8.5, although their geographical patterns were in general good agreement (Supplementary Fig. 8). Defining thermal tolerances for marine ectotherms based on their distribution ranges is a reasonable approach in the absence of empirical data because they are mainly thermal range conformers[35] (that is, they tend to occupy fully their potential thermal niche). However, we still know very little about the actual contribution of natural variability towards their thermal tolerance limits. Irrespective, because empirical estimates of physiological thermal limits are themselves prone to bias resulting from plasticity to environmental constraints[36], no approach is likely to give the true answer.

Climate niche trajectories and redistribution of species. Given the realized thermal niche of a species i at time t (N_i^t), defined by its current distribution (D_i^t) and assumed to be equal to its potential thermal niche, its distribution at the end year of the simulation period (D_i^{t+n}) was calculated as follows (Supplementary Fig. 4). We estimate the new location of the thermal niche (N_i^{t+n}) by projecting each 1° cell contained within N_i^t in the direction and speed dictated by the corresponding cell velocities. We then define the new potential distribution for the species comprising the old (N_i^t) and new (N_i^{t+n}) locations of the thermal niche, together with all those intermediate cells used to reach N_i^{t+n} from N_i^t (Supplementary Fig. 4a), thereby explicitly accounting for climate connectivity. Next, we estimate the final realized distribution of the species (D_i^{t+n}) by checking each cell within its potential distribution range against corresponding habitat and thermal filters. The presence cells were first checked for habitat suitability (Supplementary Fig. 4b), depending initially on whether species were predominantly oceanic or sublittoral/littoral neritic. Neritic species ($n = 11{,}462$) found primarily over continental or island shelves were defined as species with $\geq$75% of their current distribution within limits of the marine ecoregions of the world (MEOW) proposed by Spalding and colleagues[37]. These ecoregions cover all coastal and shelf waters shallower than 200 m with a minimum offshore threshold of 370 km. We further divided neritic species into sublittoral ($n = 3{,}100$) and littoral ($n = 8{,}362$), defined as species having $\geq$90% of their range in maritime coastline cells, to capture species dependent on proximity to strictly littoral habitats. Cells from the initial distribution of neritic species falling outside habitat boundaries ($1 \pm 3.3\%$; mean $\pm$ s.d.) were therefore not projected and excluded from the analysis. The remaining species were classified as oceanic species ($n = 1{,}334$) with no particular habitat restriction in terms of occupancy. A comparison between the thermal tolerance limits of the species (defined from the max/min SST baseline climatology) and the cell-specific environmental temperature extremes gave thereafter an estimation of thermal occupancy with the following four outcomes for local warming (Supplementary Fig. 4d where thermal comparisons are reversed for a locally cooling area): range contraction from areas at present occupied from which the species is extirpated as maximum temperature extremes exceed its upper thermal tolerance; distribution stasis corresponding to areas where the species was originally found and that remain within the thermal tolerance limits for the species; range expansion as areas at present not occupied and becoming thermally suitable for the species; and thermal intolerance as new cells occupied by the thermal niche that the species can, however, not colonize because the minimum temperature extreme is below its lower thermal tolerance. Note that because climate velocities and thermal niches are based on mean annual SST, whereas thermal suitability is estimated from absolute mean monthly maximum and minimum SST, it is possible for part of the new thermal niche to be unsuitable owing to the minimum temperature extremes being below the lower thermal tolerance for the species. The resulting new distribution (D_i^{t+n}) defines the new thermal niche for projection into the next climate change period.

Species' thermal niche trajectories were projected as in Burrows *et al.*[3] by forward iteration of each 1° SST cell centroid within a species distribution range at 0.1-year time steps throughout the corresponding climate change period. Displacement at each time step was determined from the speed and direction of local grid-cell climate velocity and considering the limitation to movement imposed by land[3].

Changes in projections resulting from the underlying variability in SST amongst climate models were assessed by comparing resulting richness patterns using the 25 and 75% quantile model ensembles against those obtained from the mean ensemble for each time period and RCP (Supplementary Fig. 6). Despite existing variability in both the magnitude and the sign of biodiversity changes across different ensembles (see the different values corresponding to the 10% cell percentiles in Supplementary Fig. 6), importantly, resulting global richness patterns were highly consistent.

Partitioning of temporal beta diversity. To estimate the contribution of temporal turnover (species replacement via co-occurring loss and gain) and nestedness (species loss or gain leading to one community being a subset of the other) towards resulting (2006–2100) cell-based changes in community composition, we applied

the additive partitioning of total beta diversity proposed by Baselga[38] for pairwise comparisons:

$$\beta_{sor} = \beta_{sim} + \beta_{sne} = \frac{b+c}{2a+b+c} = \frac{2b}{2b+a} + \left(\frac{c-b}{a+b+c}\right)\left(\frac{a}{2b+a}\right)$$

where β_{sor} refers to the total β-diversity calculated as Sørensen dissimilarity between the communities of a single cell at the start and end of the projection, accounting for both true turnover and nestedness, β_{sim} is the Simpson dissimilarity influenced only by turnover, and β_{sne} is the remaining nestedness component of β_{sor}. Between the two assemblages, a is the number of shared species and b and c refer to the number of unique species in the poorest and richest communities, respectively. Both components are bound by the value of total beta diversity, and vary in a similar way between 0 (no nestedness/turnover) and 1.

Spatial homogenization in community composition. Spatial homogenization was calculated as cell-based Sørensen dissimilarity between local communities (that is, individual 1° cells) and the corresponding regional species pool defined by all the species present within each single Marine Ecoregions of the World (MEOW) realm. Open-ocean cells falling outside realm borders were classified as High Seas and analysed separately. Differences between dissimilarities at the beginning (2006) and end (2100) of the projected period were used as an estimate of the expected extent of spatial homogenization experienced by present-day communities over the course of the century under both RCPs.

Comparison with the cumulative human impact (CHI) index. We used the new revised version[7] of the CHI. The index remains conceptually the same as its original version[8], although values are not directly comparable because two new stressors (sea level rise and light pollution) have been added to the initial list of 17. CHI values for each EEZ and sovereign region were calculated from the original values as cell-averages (weighted by EEZ area for regions). Although the CHI includes an SST anomaly component, both analyses provide different complementary information: the CHI accounts for contemporary impacts produced by human activities, of which anthropogenic climate change is an intrinsic component, to specific localities (that is, spatially static), whereas our model, based on projected isotherm movement, provides dynamic information about expected future biodiversity changes across space. Results obtained from comparing our model output to the CHI without its SST component revealed consistency in global patterns at the EEZ level (Supplementary Fig. 9 and Supplementary Table 3).

Supplementary discussion. Our bioclimatic envelope model relies on a series of key assumptions that require further comment. (1) The central assumption of our model is that SST is the primary component of a species' climate niche, which it seeks to maintain over time. This is a widely supported notion[10,11,35]. We further assume that climate migrants will track their shifting thermal niches in the direction and at the rate dictated by local climate velocity. Supporting evidence on this assumption, although less established because of the relatively novelty of the climate velocity concept, is also strong[12,16] and, importantly, robust to differences in life history[12]. Despite the general sensitivity of the distribution of marine species to global warming[11,12], not all species will need to, or be able to, track their shifting thermal niches, and even when doing so they might show a lagged response[16], which will undoubtedly affect range dynamics. (2) By inferring changes in species distribution from shifts in thermal niche space, we have purposely omitted many other important biotic, abiotic and anthropogenic drivers. Ocean acidification is, for example, another global stressor expected to influence marine biodiversity strongly under future anthropogenic climate change. Because pH and the solubility of carbonate are naturally lower at higher latitudes owing to the lower water temperatures, distribution shifts responding to ocean acidification (towards the equator) could be expected to counter those elicited by warming (polewards)[39]. However, unlike for temperature, evidence linking changes in species distribution with on-going ocean acidification is lacking, and the long-term response of marine populations to ocean acidification remains uncertain. Because projections from species distribution models are highly sensitive to the choice of predictor variables[40], the trade-off between model complexity and applicability is dependent on an adequate understanding of the factors driving that variation. Where this understanding is not available, simple models based on the fundamental relationships between key environmental variables and species distributions provide important insight into global biodiversity conservation. (3) Our model includes only projected global mean SST, because this is the only temperature parameter that is readily available from the global climate models for the temporal span and scenarios used in our analysis. Other temperature parameters might be better predictors of range shift responses to anthropogenic climate warming by better reflecting the thermal environment of the species (for example, sea bottom temperatures for benthic species), or the limiting conditions governing range dynamics (that is, temperature extremes). (4) Nevertheless, the velocity of climate change is ultimately a physical metric defining the speed and direction of change in isotherms over time and across space. Therefore, a distinction needs to be made between thermal shifts and the resulting redistribution of a species range. Although we look at the movement of thermal niches as opportunities for a species to expand, areas from which the current thermal niche shifts away are left vacant by the species only if they become thermally unsuitable. In this way we reflect the fact that range contractions promoted by climate change are often slower than expansions of the leading edge[11] because they are driven primarily by extirpation of subpopulations as conditions surpass their tolerance limits. (5) Spatial predictions of distribution range from point occurrence data (for example, AquaMaps maps) based on estimates of environmental preferences can be influenced by bias in sampling effort as well as by the selection of variables used to estimate the environmental envelopes, potentially leading to unrealistic distributions. Although it is obvious that predictions can be improved using better data (presence/absence) or increasing the sophistication of the models, this can be done only on a case-by-case basis and it is unfeasible where the objective is to analyse multi-taxon range shifts and global biodiversity patterns in the ocean. Therefore, given the resources at present available, these limitations must be accepted and acknowledged. AquaMaps represents the most comprehensive data set of species distributions globally for marine species, frequently used for global projections of commercial fish and invertebrate species richness[5,6]. AquaMaps has also been demonstrated to perform well against alternative presence-only species distribution models in the generation of species range maps[41], and show high levels of agreement with other independently derived global analysis of species richness[33], using a nearly identical set of species to that used for the present study. (6) Movement of neritic climate migrants in our model is restricted by depth as well as by geographical limits[3]. Although many of these coastal species have larval stages capable of dispersing long distances and traversing open waters, the extent to which their populations are demographically open is a subject of current debate[42]. We consider larval dispersion to be primarily passive, driven by factors (for example, currents) other than a direct response to climate change. (7) Although depth and coastal affinity might not reflect strict habitat requirements but simply covary with other biophysical factors, they are two parameters commonly used to parameterize species distribution models for global analyses[5,6]. When there is little knowledge of the suite of environmental covariates for each individual species considered, projections made without depth and coastal affinity result in more uncertain and unrealistic projections. (8) The cumulative human impact index proposed by Halpern *et al.*[7,8] has a climate change element which includes SST (although note that these are anomalies not means); however, their index refers to past (1985–2005) impacts, whereas our projections are based on climate change velocity calculated from future SSTs (2006–2100). The lack of a temporal overlap between the temperature parameters therefore minimizes the effect of a possible confounding effect. Further, we believe that crossing both effects is important for gaining better insight into future conservation and climate-change adaptation needs. The human impact index refers to local cumulative impacts and is thus spatially static (that is, related to a specific location or cell), whereas our projections of biodiversity change are based on range shifts and therefore emphasize climate connectivity (that is, movement of species in response to future climate warming).

References

32. Verbesselt, J., Hyndman, R., Newnham, G. & Culvenor, D. Detecting trend and seasonal changes in satellite image time series. *Remote Sens. Environ.* **114,** 106–115 (2010).
33. Selig, E. R. *et al.* Global priorities for marine biodiversity conservation. *PLoS ONE* **9,** e82898 (2014).
34. Stevens, G. C. The latitudinal gradient in geographical range: How so many species coexist in the tropics. *Am. Nat.* **133,** 240–256 (1989).
35. Sunday, J. M., Bates, A. E. & Dulvy, N. K. Thermal tolerance and the global redistribution of animals. *Nature Clim. Change* **2,** 686–690 (2012).
36. Denny, M. W. & Dowd, W. W. Biophysics, environmental stochasticity, and the evolution of thermal safety margins in intertidal limpets. *J. Exp. Biol.* **215,** 934–947 (2012).
37. Spalding, M. D. *et al.* Marine ecoregions of the world: A bioregionalization of coastal and shelf areas. *Bioscience* **57,** 573–583 (2007).
38. Baselga, A. Partitioning the turnover and nestedness components of beta diversity. *Global Ecol. Biogeogr.* **19,** 134–143 (2010).
39. van Hooidonk, R., Maynard, J. A., Manzello, D. & Planes, S. Opposite latitudinal gradients in projected ocean acidification and bleaching impacts on coral reefs. *Glob. Change Biol.* **20,** 103–112 (2014).
40. Synes, N. W. & Osborne, P. E. Choice of predictor variables as a source of uncertainty in continental-scale species distribution modelling under climate change. *Glob. Ecol. Biogeogr.* **20,** 904–914 (2011).
41. Ready, J. *et al.* Predicting the distributions of marine organisms at the global scale. *Ecol. Model.* **221,** 467–478 (2010).
42. Cowen, R. K. & Sponaugle, S. Larval dispersal and marine population connectivity. *Annu. Rev. Mar. Sci.* **1,** 443–466 (2009).